Adıyaman University
Journal of Engineering Sciences
Adyü J Eng Sci 2025;12(25):1-19
Adıyaman Üniversitesi
Mühendislik Bilimleri Dergisi
Adyü Müh Bil Derg 2025;12(25):1-19
Research Article / Araştırma Makalesi
DOI: 10.54365/adyumbd.1548867

Modeling of the Load and Deflection Response of Concrete Deep Beams Reinforced with Frp Bars

Frp Donatılı Derin Betonarme Kirişlerin Yük Ve Sehim Kapasitelerinin Modellenmesi

Merve Ete[1*], Abdulkadir Çevik[1]

[1] Gaziantep University, Faculty of Engineering, Departmen of Civil Engineering, Gaziantep/Türkiye

Abstract

Construction sector is developing in the same direction with technological developments. Thanks to these developments, we meet new designs. Examples for these designs are FRP (Fiber Reinforced Polymer) composites can be shown. It has become a preferred material in the construction sector due to its many benefits such as being resistant to corrosion, having high tensile strength and showing resistance to chemicals. In this study, the load and deflection at the midpoint of the span for 53 simple deep beams, reinforced longitudinally with FRP rods, were calculated (this analysis was derived from the research presented in reference number 10 in the literatüre). In section 7, new formulas suggested (equation 39 and 40) for load and deflection of RC deep beams with FRP and those formulas were derived using Eureqa, which is a symbolic regression program. The suggested formulas are compared with other methods in the existing literature. According to the comparison results, it has been determined that the real-life applicability of the suggested new formulas are higher and gives more accurate results compared to other studies

Keywords: *FRP Reinforcement, Deep Reinforced Concrete Beam, Load, Deflection*

Öz

Yapı sektörü teknolojik gelişmelerle birlikte aynı doğrultuda gelişim sergilemektedir. Bu gelişmeler sayesinde her geçen gün yeni tasarımlar ile tanışmaktayız. Bu tasarımlara FRP (Fiber Reinforced Polymer yani Lif Takviyeli Plastik) kompozitlerini örnek olarak gösterebiliriz. Korozyona karşı dirençli olması, çekme dayanımının yüksek olması ve kimyasal maddelere karşı direnç göstermesi gibi faydalarından dolayı yapı sektöründe oldukça tercih edilen bir malzeme haline gelmiştir. Bu çalışmada FRP çubuklar yardımı ile uzunlamasına güçlendirilen 53 adet basit mesnetli derin kirişlerin nihai aşamadaki yük ve orta açıklık sapması hesaplanmıştır (bu analiz literatürde 10 numaralı referansta sunulan makaleden elde edilmiştir). Ek olarak bölüm 7'de, FRP RC derin kirişlerin yük ve sapması için yeni formüller önerilmiş (denklem 39 ve 40) ve bu formüller, sembolik bir regresyon programı olan Eureqa kullanılarak türetilmiştir. Önerilen formüller, mevcut literatürdeki diğer yöntemlerle karşılaştırılmıştır. Karşılaştırma sonuçlarına göre, önerilen yeni formüllerin gerçek hayattaki uygulanabilirliğinin diğer çalışmalara kıyasla daha yüksek olduğu ve daha doğru sonuçlar verdiği tespit edilmiştir

Anahtar Kelimeler: *FRP Donatı, Derin Betonarme Kiriş, Yük, Sehim*

* Corresponding e-mail (Sorumlu yazar e-posta): me11476@mail2.gantep.edu.tr
Received (Geliş Tarihi):12.09.2024, **Accepted (Kabul Tarihi):** 13.10.2024

1. Introduction

Reinforced concrete (RC) deep beams are often used for transfer girders, bridge cap beams, and pile-supported foundations [1]. The corrosion of steel reinforcement bars in reinforced concrete buildings within severe environments has emerged as a major factor contributing to concrete degradation, leading to reduced service life and expensive repairs [2].

Due to such problems in reinforced concrete structures, the use of fiber reinforced polymer (FRP) reinforcements, which is a corrosion resistant material, has emerged as an alternative solution method. It has started to be used because of its advantages such as lightness, high strength, corrosion resistance, high fatigue strength, low thermal conductivity and lack of magnetic permeability [3-4].

2. FRP bars

The usage of FRP composites in the construction industry first started for the purpose of strengthening the building elements, and then its usage areas have expanded and it is rapidly moving towards being an alternative to existing building materials [5]. FRP bars have lower weight, lower Young's modulus, and stronger strength than steel bars. The three types of fiber that are most frequently used are aramid (AFRP), glass (GFRP) and carbon (CFRP).

2.1. Types of FRP bars

FRP bars are made of different fibres (glass, carbon and aramid). The kind and shape of the surface of FRP bars may significantly vary from those of deformed steel bars. Diverse surface profiles entail varying bonding processes and causes of failure. [6].

GFRP (glass fiber reinforced polymer) bars has advantages such as resistance to corrosion, lightness, high strength, being able to give the desired shape, high fatigue resistance, low thermal conductivity properties. However, it has disadvantages such as low E-modulus, dependence of strength on fiber direction, brittle material properties, problems in adherence and clamping due to the flat surface, and being expensive [7].

AFRP (aramid fiber reinforced polymer) bars have secured a lasting and expanding presence in the construction sector due to their advantageous mechanical properties and endurance, particularly in the reinforcement of reinforced concrete elements [8]. Its specific gravity is 6 times less than steel. In addition, its modulus of elasticity is 4 times lower compared to steel. This provides advantages such as less losses due to the shrinkage and creep of the concrete and the need for during the initial stretching, the tendon extended farther.

CFRP (carbon fiber reinforced polymer) bars are dimensionally stable, resist moisture and many chemicals due to their chemical content, and have high electrical/thermal conductivity. The most important disadvantage of carbon fibers for the user is that the composite color cannot be preserved as desired due to its black color. Another disadvantage is the high cost. Carbon fibers have a strong but light structure [7].

3. Proposed study

In this chapter proposed formulas are sourced from reference [10] and showed as follows:

A modified version of study developed by Lu [9] to use concrete beams with steel reinforcement is used to forecast the midspan deviation associated with various loading stages in deep FRP RC beams [10]. This proposed study [10] was created using test results from totally 53 beams that underwent 4-point bending and were documented in the literature 11-16.

$$\mathbf{\Delta = \Delta s + \Delta f} \quad (1)$$

Where, Δ is total deflection, Δ_s and Δ_f are eflections deflections resulting from shearing and bending, respectively.

3.1. Cracking load (P_{cr})

The cracking load P_{cr} is calculated using $P_{cr,f}$ load of cracking caused by crack of flexure and $P_{cr,w}$ load of cracking caused by cracking of the web. Pcr is determined by choosing the smaller of these two cracking values. $P_{cr,w}$ is calculated using the following equation [10],

$$\mathbf{Pcr, w = \frac{4}{3} fcr, w\ b\ D} \quad (2)$$

where $f_{cr,w}$ is max tensile stress (N/m²) in beam's web, b is beam's width (mm), D is beam's depth(mm) . In accordance with IS: 1343-1980 [17] the fcr,w magnitude is calculated as [10],

$$\mathrm{fcr, w} = 0.24\sqrt{1.25f'c} \quad (3)$$

where f'_c is compressive strength of concrete (MPa). In order to calculate the load at which flexural cracking occurs ($P_{cr,f}$) equation in below [10],

$$\mathrm{Pcr, f} = \mathrm{Mcr}\ \frac{2}{\alpha} \quad (4)$$

where α is shear span lenght. According to Dischinger's model [18], M_{cr} is cracking moment determined by following Equation 5 [10],

$$\mathrm{Mcr} = \alpha\ \mathrm{ft}\ \frac{\mathrm{Ig}}{\mathrm{ymax}} \quad (5)$$

where I_g is gross moment of inertia.

f_t (stress of cracking) is provided by IS:456 [19] and it is calculated by equation in below [10],

$$\mathrm{ft} = 0.7\sqrt{1.25f'c} \quad (6)$$

α in Equation (5) is given by [10]

$$\alpha = \begin{cases} 0.46\frac{1}{D}0.55;\ when\ 1 \le \frac{1}{D} \le 4 \\ 0.46;\ when\ \frac{1}{D} < 1 \end{cases} \quad (7)$$

3.2. Ultımate load (P_u)

$$\mathbf{Pu = 2. Vu} \quad (8)$$

where P_u is ultimate load. According to Hwang and Lee [20], Ultimate shear strength V_u is calculated by following Equation 9 [10],

$$V_u = (k_h + k_v - 1)\xi\,(f'c\,Astr)\sin\theta \quad (9)$$

where k_h is reinforcement index in horizontal, k_v is reinforcement index in vertical and k_v is equal to 1. ξ is softening factor. A_{str} is effective section of diagonal strut. Θ is inclination angle.

$$\boldsymbol{\xi} = \frac{\mathbf{3.35}}{\sqrt{\mathbf{f'c}}} \leq \mathbf{0.52} \quad (10)$$

$$k_h = \mathbf{1} + (\bar{k}_h - \mathbf{1})\frac{\mathbf{Af\ fp}}{\mathbf{Fh}} \leq \bar{k}_h \quad (11)$$

where $\overline{kh}$ is the highest permissible value of k_h. Af is FRP bar's area in tensile region. f_p is FRP bar's tensile strength. F_h is horizontal force of tension.

$$\bar{k}_h = \frac{1}{1-0.2(\gamma h-\gamma h2)} \quad (12)$$

where γh is horizontal factor of shear.

$$\gamma h = \frac{2\tan\theta - 1}{3}\ \text{, but } 0 \leq \gamma h \leq 1 \quad (13)$$

$$\theta = \tan - 1\left(\frac{jd}{a}\right) \quad (14)$$

where, as shown in Figure 1 (the datas presented in this figure are sourced from article number [10] in the literature), the distance between compressive force C and tensile force T is called as jd [10].

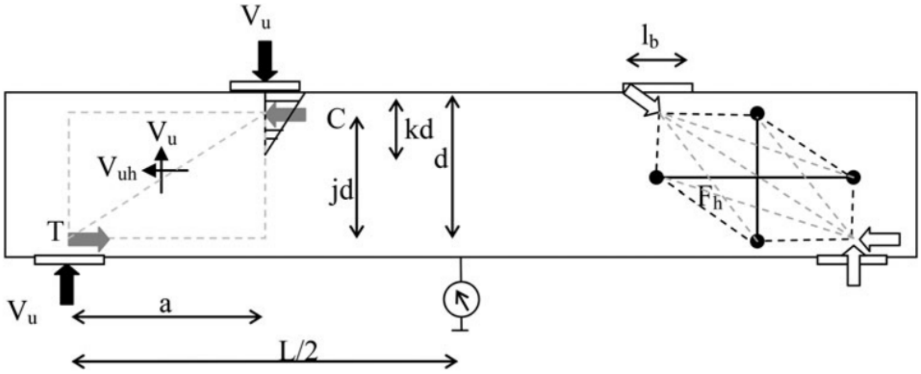

Figure 1. Model of the Internal Forces with Softened Strut and Tie [10]

$$\mathbf{jd} = \mathbf{d} - \frac{\mathbf{kd}}{\mathbf{3}} \quad (15)$$

where d is effective beam depth, kd is compression zone depth, L is deep beam span.

$$k = \sqrt{[m\rho + (m-1)\rho']^2 + 2\left[m\rho + \frac{(m-1)\rho' d'}{d}\right]} - [m\rho + (m-1)\rho']\ ;\ 0 \leq k \leq 1 \quad (16)$$

where k is natural axis coeff. ρ' is compression reinforcement ratio. d' is a compression zone that provides cover of effective.

$$m = \frac{Ef}{Ec} \tag{17}$$

where E_f elasticity modulus of bars, Ec elacticity modulus of concrete. The ratio of the tension zone's longitudinal FRP reinforcement is denoted as ρ in Equation (16), and it is calculated as follows [10]

$$\boldsymbol{\rho} = \frac{\mathbf{Af}}{\mathbf{bd}} \tag{18}$$

$$\rho' = \frac{Af'}{bd} \tag{19}$$

where A_f' is FRP bar's area in compression region.

$$\overline{Fh} = \gamma h \ x \ \overline{kh} \ \xi \ (f'c \ Astr) \ x \cos\theta \tag{20}$$

where $\overline{Fh}$ is horizontal concrete force. According to Lu [9], A_{str} is given by [10],

$$Astr = bs \ x \ ts \tag{21}$$

where b_s is strut width, t_s is strut thickness.

$$ts = \sqrt{(kd)2 + Ib\string^2} \tag{22}$$

where I_b is the upper sided loading plate's width.

$$Vu = kh \ \xi \ (f'c \ Astr) \sin\theta \tag{23}$$

β_s is factor of strut efficiency. Equation (23) is adjusted to become Equation (24) in this purposed study [10].

$$Vu = \beta s \ kh \ \xi \ (f'c \ Astr) \sin\theta \tag{24}$$

The regression analysis of empirical strength of shear parameter of 53 deep concrete reinforced beams made of FRP, showed in the literature [11,12,13,14,15,16] establishes the size of the effectiveness factor for strut β_s. β_s is discovered to have a value of 0.71. Equations (8) and (24) are used to calculate the shear strength and the ultimate load of the beam, respectively [10].

3.3. Calculation of the deflection caused by shear (Δ_s)

$$\Delta s = \gamma \ a \tag{25}$$

where γ is average shear strain. For the membrane components made of RC exposed to normal load and shear load, Hsu [21], Hwang and Lee [20-21], and Hwang et al. [23, 24 and 25] suggested using a two-dimensional compatibility condition [10].

$$\gamma = 2(\varepsilon r - \varepsilon d)\sin\theta \cos\theta \tag{26}$$

ε_r is principle tensile strain perpendicular to the compression strut. ε_d is the diagonal compression strut's strain. Hwang [23], suggested the equation shown below to calculate εr [10],

$$\varepsilon r + \varepsilon d = \varepsilon h + \varepsilon v \tag{27}$$

where ε_h is the horizontal tie's normal strain, ε_v is the vertical tie's normal strain. According to Hwang and Lee [22] ε_v is considered to be 0.002. Hwang [24] suggested ε_h and provided by [10],

$$\varepsilon h = \frac{Fh}{Af\ Ef} \leq \frac{fp}{Ef} \tag{28}$$

$$Fh = \gamma h\ V/\tan\theta \tag{29}$$

$$V = P/2 \tag{30}$$

ε_d from Equation (27) suggested by Zhang and Hsu [26] and is determined by [10],

$$\varepsilon d = -\xi\ \varepsilon \tag{31}$$

3.4. Calculation of the deflection caused by shear (Δs)

This proposed study [10] makes modifications to the bilinear model that was originally put forward in CP 110 [27].

$$\Delta f = \Delta f1 + \Delta f2 \tag{32}$$

$$\Delta f1 = \frac{\beta\ I\text{^}2\ M}{Ec\ Ig};\ \text{when } 0 < M \leq Mcr \tag{33}$$

where I is beam span, M is beam moment.

$$\Delta_{f2} = \begin{cases} \dfrac{\beta\ I2\ (M-Mcr)}{kf\ Ec\ Ieff};\ \text{when } M_{cr} < M < M_u \\ \\ \dfrac{\beta\ I2\ (M-Mcr)}{kf\ Ec\ Icr};\ \text{when } M_u = M \end{cases} \tag{34}$$

where I_{cr} cracked area's moment of inertia.

$$\beta = 1/24[\ 3 - 4(a/I)2\ ] \tag{35}$$

$$M = \frac{P}{2}a \quad \text{and} \quad Mcr = \frac{Pcr}{2}a \tag{36}$$

To reduce bar pullout that would result in severe beam deformation, the FRP bars in this investigation are anchored at the ends [10]. IS:456 [19] proposed I_{eff} which represents efficient moment of inertia of the beam [10],

$$\text{Ieff} = \frac{\text{Icr}}{1.2 - \frac{\text{Mcr}}{\text{M}}\frac{\text{jd}(1-\text{k})}{\text{d}}} \text{ where Icr} \leq \text{Ieff} \leq \text{Ig} \tag{37}$$

IS:456 [25] suggested I_{cr} moment of the broken concrete portion [10],

$$\text{Icr} = \frac{\text{b(kd)\^{}3}}{3} + (\text{m}-1)\text{A}'\text{f}(\text{kd}-\text{d}')^2 + \text{m Af}(\text{d}-\text{kd})\text{\^{}2} \tag{38}$$

4. Experimental program

Experimental details regarding the samples used in the database, sourced from reference [10], are provided in this chapter as follows:

By altering the ratio of reinforcement throughout the were fabricated and evaluated using a four-point testing method. Figure 2 (the datas presented in this figure are sourced from article number [10] in the literature) provides the cross-sectional schematic, beam reinforcement details, and test setup. Table 1 (the datas presented in this table are sourced from article number [10] in the literature) includes information about the beams [10].

Table 1: Specifications of the test bars [10]

Authors	Beam ID	Type of FRP	l (mm)	b (mm)	d (mm)	D (mm)	a/d	l_b (mm)	ρ_f (%)	E_f (Gpa)	f_p (Mpa)	ε_{fu} (%)	E_c (Gpa)	f'_c (Mpa)
Present Study	G6/0.50	GFRP	990	170	416	500	0.50	50	1.70	41,0	655	1.54	35.9	58.5
	G6/0.75	GFRP	990	170	416	500	0.75	50	1.70	40,0	680	1.53	36.1	59.0
	G6/1.0	GFRP	990	170	416	500	1.00	50	1.70	39,0	650	1.56	35.8	58.0
	G4/0.5	GFRP	990	170	416	500	0.50	50	1.14	42,0	640	1.52	35.6	57.5
	G4/0.75	GFRP	990	170	416	500	0.75	50	1.14	41,8	660	1.55	35.8	58.0
	G4/1.0	GFRP	990	170	416	500	1.00	50	1.14	41,0	645	1.57	36.4	60.0

The datas presented in this table are sourced from article number [10] in the literature.

The beams were cast, cured with wet burlap for 28 days, evaluated using a digital beam 1000 kN with a four - point loading setup with 25 kN increments at a 0.250 kN/s rate. The loads were measured with a load cell, deflection by dial gauges, and strain in the FRP bars with electrical strain gauges at mid-span. Concrete strain was measured by demec gauges. Testing data was recorded through a multi-channel system, which captured load and mid-span deflection; reports included the final phase loads and initial cracks. Figures 3 (a) to (d) provide images of the construction phases and beam testing [10].

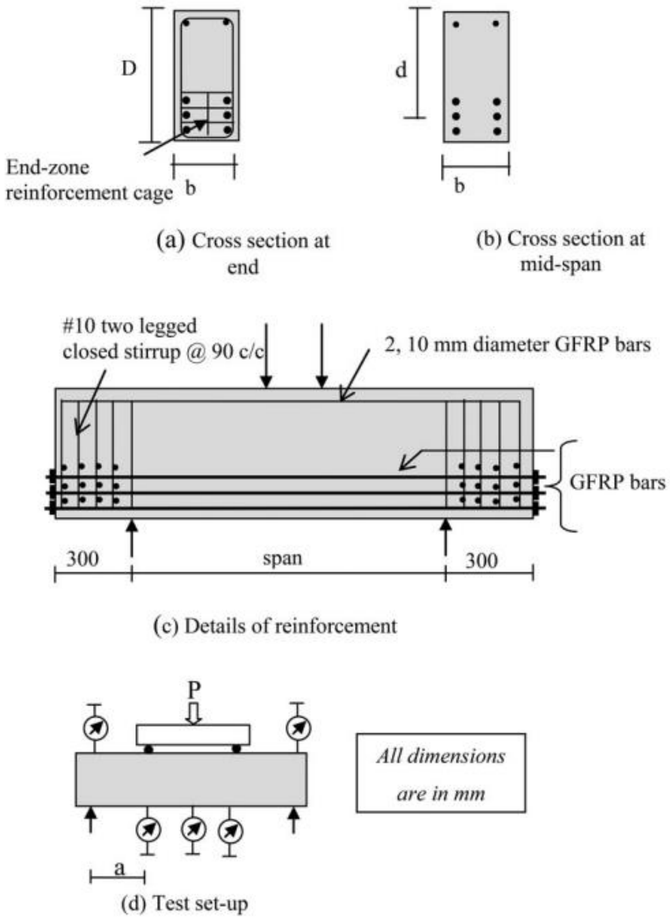

Figure 2: Information about the test set-up and test beam [10]

(a)Reinforcement cage of the beam

(b) Reinforcement cage at the end zone

(c)End anchorage of the longitudinal bars

(d)Position of Location of Dial gauges

Figure 3: Construction phases of the testing beams [10]

5. Discussion the results of experimental program

The datas presented in this section are sourced from article [10] in references.

Deformations were seen to be gradual during the first phases of load in all six beams. Response of deflection of the broken beam is discovered to be nonlinear throughout the succeeding loading stages. As compared to beams with four longitudinal bars, the longitudinal bars of the six-bar beams have a smaller deflection of middle span. For beams with a lower ratio of a/d, the deflection of mid-span discovered as smaller. At the beam's tension face, fractures first appeared. Later steps in the loading process, it was seen that the diagonal crack's breadth increased. The transverse shear caused the beams to fail. The reduction in the shear span to depth (a/d) ratio was shown to greatly boost the GFRP beam's load carrying capability. With increasing (a/d) ratio, it was discovered that the mid span deflection was increasing as well. Figure 4 displays beam cracks at the point of fail. All of the study's specimens experienced a similar failure mechanism [10].

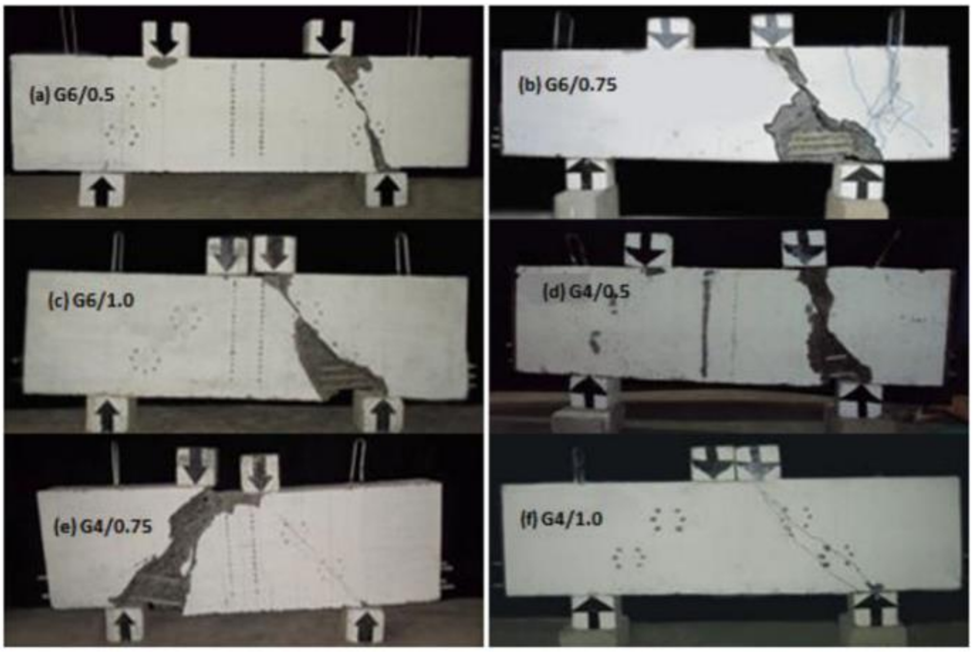

Figure 4: Testing beams' cracking model and fail mechanism [10]

6. Estimated and experimental test values analysis

The datas presented in this section are sourced from article [10] in references.

Table 2 (the datas presented in this table are sourced from article number [10] in the literature) compares predicted and experimental loads at initial cracking and final stages. The mean ratio of experimental to predicted strength ($P_{cr,e}/P_{cr,p}$) is 0.99 at initial cracking (variation coefficient 7.07%) and 1.13 at the final stage (variation coefficient 3.54%). The proposed study [10] accurately estimates both ultimate (final) stages and first cracking load.

Table 2: Comparing testing sample's estimated and experimental loads at the first step of cracking phase and ultimate (final) phase [10]

			At first Cracking stage			At ultimate stage			
Authors	Beam ID	Type of FRP	$P_{cr,e}$ (kN)	$P_{cr,p}$ (kN)	$P_{cr,e}/P_{cr,p}$	$P_{u,e}$ (kN)	$P_{u,p}$ (kN)	$P_{u,e}/P_{u,p}$	Type of Failure
Present Study	G6/0.50	GFRP	250	233	1.07	900	757	1.19	D.S.
	G6/0.75	GFRP	170	183	0.93	550	508	1.08	D.S.
	G6/1.0	GFRP	130	136	0.96	460	404	1.14	D.S.
	G4/0.5	GFRP	250	231	1.08	760	681	1.12	D.S.
	G4/0.75	GFRP	170	181	0.94	520	457	1.14	D.S.
	G4/1.0	GFRP	130	138	0.94	410	371	1.11	D.S.
Mean					0.99			1.13	
S.D.					0.07			0.04	
CoV (%)					7.07			3.54	

The datas presented in this table are sourced from article number [10] in the literature.

Table 3 (the datas presented in this table are sourced from article number [10] in the literature) compares anticipated and empirical deflections at initial cracking and ultimate stages. The ratio of experimental to predicted deflection ($\Delta_{cr,e}/\Delta_{cr,p}$) at initial cracking is 0.75 with a CoV of 6.67%. At the ultimate stage, the ratio ($\Delta_{u,e}/\Delta_{u,p}$) is 0.88 with a CoV of 5.68%. These results indicate the proposed study [10] accurately estimates deflections at both stages.

Table 3: Testing sample's deflections of estimated and experimental at initial stage of cracking and at the ultimate (final) stage [10]

			At first Cracking stage			At ultimate stage			
Authors	Beam ID	Type of FRP	$\Delta_{cr,e}$ (mm)	$\Delta_{cr,p}$ (mm)	$\Delta_{cr,e}/\Delta_{cr,p}$	$\Delta_{u,e}$ (mm)	$\Delta_{u,p}$ (mm)	$\Delta_{u,e}/\Delta_{u,p}$	Type of Failure
Present Study	G6/0.50	GFRP	0.41	0.50	0.82	3.10	3.40	0.91	D.S
	G6/0.75	GFRP	0.46	0.66	0.70	3.21	3.94	0.81	D.S
	G6/1.0	GFRP	0.51	0.71	0.72	3.62	4.37	0.83	D.S
	G4/0.5	GFRP	0.51	0.63	0.81	3.51	3.95	0.89	D.S
	G4/0.75	GFRP	0.58	0.79	0.73	4.11	4.43	0.93	D.S
	G4/1.0	GFRP	0.62	0.85	0.73	4.32	4.88	0.89	D.S
Mean					0.75			0.88	
S.D.					0.05			0.05	
CoV (%)					6.67			5.68	

The datas presented in this table are sourced from article number [10] in the literature.

The proposed model [10] was used to project 53 beams' load and deflection. It is possible to estimate 53 FRP-RC deep beams' strength via studies from literature [28,29,30,31,32] and with the help of study called as 'strut and tie' which suggested from ACI 318 [33]. 53 FRP-RC beams' experimental and predicted strengths are contrasted in Table 4 (the datas presented in this table are sourced from article number [10] in the literature). By a CoV of 36.3%, the average value of ($P_{u,e}/P_{u,p}$) which represents experimental to estimated ultimate (final) load for 53 pieces of beams was determined as 0.89, which is consistent with the model suggested by ACI-318 [33]. Using the models suggested by [28-32] it is discovered that mean (average) value of the ratio of the experimental to the estimated ultimate (final) load ($P_{u,e}/P_{u,p}$) is moderate. When proposed model [10] was used to forecast the ($P_{u,e}/P_{u,p}$) ratio, it was discovered that the mean value of 53 beams was 1.05, with a coefficient of variation of 29.5%.

Tables 5 and 6 (the datas presented in these tables are sourced from article number [10] in the literature) compares the deflection of 53 pieces of FRP reinforced concrete beams' final stages via empirical and estimated data from different publications [34, 35, 36, 37, 38, 39] and the current codes [28, 32, 40, 41].

For 53 beams the proposed model [10] was found to have a CoV 40.80% and a value of mean as 1.03 for empirical to the estimated deflection ratio ($\Delta_{u,e}/\Delta_{u,p}$) at final stage. It was discovered that the value of $\Delta_{u,e}/\Delta_{u,p}$ was varying 0.340 to 2.140. Value of ratio $\Delta_{u,e}/\Delta_{u,p}$ was determined for amount of 34 beams, to be lower than 1.0 with a ratio of a/d below 1.00 out of 53 test data utilized in this investigation. This suggests that when a/d ratio is lower than 1.00, the deflection is overstated by the proposed study [10]. This could be because the arching effect has a reducing effect on bending and shearing-related deformation.

In table 5 (the datas presented in this table are sourced from article number [10] in the literature) the mean 1.03, that matches with the proposed study [10], is lower than the mean of ($\Delta_{u,e}/\Delta_{u,p}$) for other models [34, 35, 36, 37, 38, 39] which was found to be in the range of 1.28 to 2.04 for those models. The proposed study's [10] CoV of estimation was determined as 40.80%. On the other hand for other studies CoV value is ranging from 27.6% to 33.9%. It was discovered that other studies existing to determine the deflection of FRP RC beams were extremely conservative. In light of this, that may said the proposed model's [10] estimation of final step of FRP deep reinforced concrete beams deflection and strength is comparable to the convenient empirical outcomes.

7. Numerical study modeling

Accurate measurement of ultimate load and deflection is essential for assessing structural condition and determining necessary improvements. This study introduces new formulas for these measurements, developed using scientific approaches and engineering standards from the literature. These formulas aim to provide precise and comprehensive results, contributing to the field. The results will be compared with existing studies, application codes, and the study's predictions, using the symbolic regression method in accordance with Eurocode standards.

7.1. Suggested Formula for Determining Load

For the ultimate load capacity (P_u), the newly proposed formula is presented below in the Numerical Study Modelling (NSM) section:

$$\mathbf{(Pu) = 0.896 * D * 0.405(a/d)\ \log\sqrt{0.013 * b}\ \sqrt{0.013 * b * 0.0624 * \rho f * fp}} \quad (39)$$

where ρf represents the reinforcement ratio of the FRP bars.

Table 7 (the datas presented in this table are sourced from article number [10] in the literature) compares the estimated and experimental ultimate loads of 53 FRP-RC beams using the new formula from the Numerical Study Modelling (NSM) section, current application codes, and existing studies. Additionally, results from Equation 39 for these beams are listed in the 'NSM (Equa. 39)' column in Table 7.

According to the results presented in Table 7; the mean Pu,e/Pu,p ratio for 53 FRP-RC beams is 0.89 with a CoV of 36.3% for ACI-318 [33]. Other studies [28,29,30,31,32], $P_{u,e}/P_{u,p}$ ratios ranging from 1.6 to 5.13, with CoV values of 25.6% to 41.7%. The proposed study's [10] Equation 8 yields a mean ratio of 1.05 with a CoV of 29.5%. Equation 39 from the NSM section, with a mean ratio of 2.48 and a CoV of 19.57%, offers superior accuracy and reliability, closely aligning with actual structural behavior.

7.2. Suggested Formula for Determining Load

For the ultimate stage total deflection ($\Delta_{u,e}$), the newly proposed formula is presented below in the Numerical Study Modelling (NSM) section:

$$\mathbf{\Delta} = \frac{\mathbf{L}\sqrt{\mathbf{Ec}\sqrt{\frac{98.6*\mathbf{d}*\mathbf{L}*\mathbf{E}c\sqrt{\frac{\mathbf{D}}{(\rho \mathbf{f})*\mathbf{E}f}}}{b*\mathbf{E}f}}}}{\mathbf{D}(\mathbf{f'c})} \tag{40}$$

Table 8 (the datas presented in this table are sourced from article number [10] in the literature) compares the predicted and experimenta; ultimate loads of 53 FRP-RC beams using the new formula from the Numerical Study Modelling (NSM) section, current application codes, and existing studies. Results from Equation 40 for these beams are also shown in the 'NSM (Equa. 40)' column of Table 8.

According to the results presented in Table 8, the Proposed Study's [10] Equation 1 yields $\Delta u,e/\Delta u,p$ ratio of 1.03 with a CoV of 40.80%. Current codes and studies [28,32,40,41] shows $\Delta u,e/\Delta u,p$ ratio between 1.90 and 2.03, with CoV values from 33% to 34%. Other studies [35,36,37,38,39] report a $\Delta_{u,e}/\Delta_{u,p}$ ratio between 1.28 and 2.04, with CoV values from 32.5% to 33.9%. Equation 40 from the NSM section gives a $\Delta_{u,e}/\Delta_{u,p}$ ratio of 1.04 with a CoV of 26.99%. Equation 40 from the NSM section outperforms existing formulas and studies, proving to be more effective and reliable. Its low CoV value indicates less variability and closer alignment with actual structural behavior, confirming its accuracy.

8. Conclusion

Vertical deflections at the mid span and loading point are similar, indicating uniform deflection along the beam. Experimental results align well with predicted load and deflection of RC deep beams with FRP, confirming model reliability. An increase in beam depth reduces normalized shear stress, showing sensitivity to geometric parameters. During initial breaking, shear deflections account for 89% to 95% of total deflection, while in the final phase, they contribute 42% to 58% of overall displacement, highlighting their significant impact on beam behavior [10].

New formulas (equation 39 and 40) for load and deflection of RC deep beams with FRP proposed in Section 7 were derived using Eureqa, which is a symbolic regression program. They were compared with existing results and this comparison showed that the new formulas better reflect reality, providing more accurate results in structural modeling.

Table 4: At ultimate (final) step, comparing experimental and predicted loads for test specimens via current application codes and current study [10]

													$P_{u,e}/P_{u,p}$						
Sl.No.	Beam ID	Type of FRP rebar	b (mm)	d (mm)	a/d	l_{b1} (mm)	l_{b2} (mm)	f'_c (MPa)	ρ_f (%)	E_f (Gpa)	f_u (Mpa)	$P_{u,e}$ (kN)	JSCE [29]	BISE [30]	NRC [31]	ISIS [28]	ACI 318 [33]	CSA [32]	Job Thomas & S. Ramadass [10]
1	G6/0.5 [4]	GFRP	170	416	0,5	50	50	58,5	1.7	41	655	900	10.09	8,08	7,7	9,18	1,33	1,71	1,19
2	G6/0.75 [4]	GFRP	170	416	0,75	50	50	59	1.7	40,0	680	550	6.21	4,97	4,74	5,66	0,81	1,05	1,08
3	G6/1.0 [4]	GFRP	170	416	1,00	50	50	58	1.7	39,0	650	460	5.24	4,21	4,05	4,83	0,69	0,89	1,14
4	G4/0.5 [4]	GFRP	170	416	0,50	50	50	57,5	1.14	42,0	640	760	9.65	7,78	7,35	7,74	1,14	1,62	1,12
5	G4/0.75 [4]	GFRP	170	416	0,75	50	50	58	1.14	41,8	660	520	6.61	5,32	5,02	5,28	0,78	1,11	1,14
6	G4/1.0 [4]	GFRP	170	416	1,00	50	50	60	1.14	41,0	645	410	5.25	4,17	3,93	4,13	0,59	0,87	1,11
7	G1.13 [48]	GFRP	300	1088	1,15	203	228	37	1.21	66,4	1000	2687	8.55	7,39	6,50	5,87	1,69	2,70	1,62
8	G0.83 [48]	GFRP	300	1088	0,83	203	228	38,7	1.21	66,4	1000	3000	9.40	8,12	7,10	6,41	1,33	2,41	1,36
9	G1.47 [48]	GFRP	300	1088	1,47	203	228	38,7	1.21	66,4	1000	1849	5.80	5,01	4,38	3,95	1,42	2,64	1,30
10	A3D9M-1.4 [45]	AFRP	200	250	1,40	100	100	26,1	0.38	80,6	1826,9	272,1	6.07	5,24	4,28	4,19	1,04	1,74	1,15
11	A3D9M-1.7 [45]	AFRP	200	250	1,70	100	100	26,1	0.38	80,6	1826,9	197,9	4.41	3,81	3,12	3,05	0,93	1,70	0,98
12	A3D9M-2.1 [45]	AFRP	200	250	2,10	100	100	26,1	0.38	80,6	1826,9	176	4.90	3,39	2,77	2,71	1,05	2,07	1,05
13	A4D9M-1.7 [45]	AFRP	200	250	1,70	100	100	26,1	0.51	80,6	1826,9	242	4.90	4,22	3,67	3,72	1,09	1,90	1,18
14	A5D9M-1.7 [45]	AFRP	200	250	1,70	100	100	26,1	0.64	80,6	1826,9	267,9	5.04	4,33	3,92	4,12	1,16	1,97	1,29
15	A5D9L-1.7 [45]	AFRP	200	310	1,70	100	100	26,1	0.51	80,6	1826,9	268,5	4.62	3,99	3,44	3,34	1,08	1,73	1,26
16	C3D9M-1.4 [45]	CFRP	200	250	1,40	100	100	26,1	0.38	120,2	1955,8	338,5	6.61	5,70	4,37	4,27	1,22	1,93	1,41
17	C3D9M-1.7 [45]	CFRP	200	250	1,70	100	100	26,1	0.38	120,2	1955,8	213,1	4.16	3,59	2,75	2,69	0,94	1,63	1,03
18	C3D9M-2.1 [45]	CFRP	200	250	2,10	100	100	26,1	0.38	120,2	1955,8	105,3	2.06	1,77	1,36	1,33	0,59	1,10	0,61
19	C4D9M-1.7 [45]	CFRP	200	250	1,70	100	100	26,1	0.51	120,2	1955,8	192,2	3.41	2,94	2,39	2,43	0,81	1,34	0,92
20	C5D9M-1.7 [45]	CFRP	200	250	1,70	100	100	26,1	0.64	120,2	1955,8	302,8	4.99	4,29	3,63	3,82	1,23	1,98	1,43
21	C5D9L-1.7 [45]	CFRP	200	310	1,70	100	100	26,1	0.51	120,2	1955,8	290,8	4.38	3,78	3,05	2,96	1,09	1,66	1,32
22	A3D9S-1.7 [45]	AFRP	200	190	1,70	100	100	26,1	0.50	80,6	1826,9	219,2	5.48	4,73	4,20	4,44	1,12	2,28	1,47
23	C3D9S-1.7 [45]	CFRP	200	190	1,70	100	100	26,1	0.50	120,2	1955,8	209,7	4.59	3,96	3,29	3,48	1,02	1,94	1,05
24	G8N6 [42]	GFRP	300	1097	1,14	130	228	49,3	0.69	47,6	790	1447	5.71	4,84	4,05	3,21	0,74	1,69	1,09
25	G8N8 [42]	GFRP	300	1088	1,15	130	228	49,3	1.24	51,9	750	1906	6.04	5,13	4,49	4,08	0,98	1,86	1,22
26	C12N3 [42]	CFRP	300	1111	1,13	130	228	38,7	0.26	120	1596	1191	5.04	4,35	2,65	1,85	0,77	1,51	1,02
27	C12N4 [42]	CFRP	300	1106	1,13	130	228	38,7	0.46	144	1899	1601	5.29	4,57	3,08	2,29	1,04	1,63	1,13
28	A1N [44]	GFRP	310	257	1,07	100	100	40,2	1.49	41,1	709	814	7.88	6,81	6,87	8,89	1,00	1,55	1,12
29	A2N [44]	GFRP	310	261	1,44	100	100	45,4	1.47	41,1	709	471	4.35	3,76	3,71	4,77	0,66	1,33	0,75
30	A3N [44]	GFRP	310	261	2,02	100	100	41,3	1.47	41,1	709	243	2.31	2,00	2,01	2,58	0,55	1,17	0,55
31	A4H [44]	GFRP	310	261	2,02	100	100	64,6	1.47	41,1	709	192	1.76	1,36	1,27	1,63	0,28	0,80	0,34
32	B1N [44]	GFRP	300	503	1,08	200	200	40,5	1.7	37,9	765	1273	7.54	6,52	6,88	7,61	0,80	1,62	0,92
33	B2N [44]	GFRP	300	501	1,48	200	200	39,9	1.71	37,9	765	799	4.76	4,12	4,35	4,83	0,68	1,64	0,75
34	B3N [44]	GFRP	300	502	2,07	200	200	41,2	1.71	37,9	765	431	2.54	2,19	2,31	2,56	0,52	1,44	0,52
35	B4N [44]	GFRP	300	496	1,48	200	200	40,7	2.13	41,1	709	830	4.48	3,87	3,97	4,82	0,69	1,55	0,75
36	B5H [44]	GFRP	300	497	1,48	200	200	66,4	2.12	41,1	709	1062	5.48	4,21	3,98	4,82	0,54	1,68	0,76
37	B6H [44]	GFRP	300	505	2,06	200	200	68,5	1.7	37,9	765	376	2.12	1,61	1,56	1,72	0,27	1,05	0,35
38	C1N [44]	GFRP	301	889	1,10	330	330	51,6	1.58	42,3	938	2269	8.24	6,88	6,53	6,42	0,68	2,14	0,87
39	C2N [44]	GFRP	304	891	1,49	330	330	50,7	1.56	42,3	938	1324	4.77	4,01	3,82	3,73	0,53	1,97	0,64
40	C-0.7/1.6 [41]	CFRP	250	326	1,69	100	100	40,5	0.78	143,0	1036	359	2.94	2,54	1,98	2,05	0,59	1,17	0,79
41	G-0.7/1.6 [41]	GFRP	250	326	1,69	100	100	40,5	0.78	43,0	776	329	4.03	3,48	3,31	3,42	0,63	1,51	0,81
42	C-1.2/1.6 [41]	CFRP	250	326	1,69	100	100	40,5	1.24	143,0	1036	390	2.74	2,37	1,92	2,22	0,64	1,10	0,80
43	G-1.2/1.6 [41]	GFRP	250	326	1,69	100	100	40,5	1.24	43,0	776	350	3.67	3,17	3,14	3,64	0,58	1,40	0,83
44	C-1.7/1.6 [41]	CFRP	250	326	1,69	100	100	40,5	1.71	143,0	1036	467	2.95	2,55	2,07	2,66	0,77	1,19	0,91
45	G-1.7/1.6 [41]	GFRP	250	326	1,69	100	100	40,5	1.71	43,0	776	392	3.69	3,19	3,17	4,07	0,64	1,42	0,90
46	C-1.2/1.3 [41]	CFRP	250	326	1,30	100	100	40,5	1.24	143,0	1036	744	5.23	4,52	3,66	4,24	0,97	1,42	1,23
47	G-1.2/1.3 [41]	GFRP	250	326	1,30	100	100	40,5	1.24	43,0	776	538	5.64	4,88	4,83	5,59	0,70	1,46	1,03
48	CF-B-1 [39]	CFRP	150	150	1,55	50	50	34,7	1.13	134,0	1180	185,2	4.77	3,72	3,32	4,27	0,90	1,73	1,45
49	CF-d-250 [39]	CFRP	150	250	1,41	50	50	41,7	1.35	134,0	1180	298,1	5.12	3,62	2,98	3,76	1,12	1,29	1,33
50	CF-d-350 [39]	CFRP	150	350	1,36	50	50	37,6	1.21	134,0	1180	468,2	6.73	4,75	3,94	4,44	1,90	1,57	1,13
51	F-B-1 [39]	GFRP	150	150	1,55	50	50	35,5	1.29	40,8	690	135,5	3.72	3,84	4,19	5,60	0,65	1,73	1,16
52	F-d-250 [39]	GFRP	150	250	1,41	50	50	42	1.39	40,8	655	243,1	5.50	4,34	4,36	5,53	0,91	1,50	1,39
53	F-d-350 [39]	GFRP	150	350	1,36	50	50	48	1.24	40,8	655	422,5	4.63	5,82	5,66	6,42	1,34	1,86	1,93
Mean													5.13	4,34	3,91	4,21	0,89	1,60	1,05
S.D													1.88	1,57	1,54	1,76	0,32	0,41	0,31
CoV													36.6	36,2	39,4	41,7	36,3	25,6	29,5

The datas presented in this table are sourced from article number [10] in the literature.

Table 5: At ultimate (final) step, comparing experimental and predicted deflection in middle-span for test specimens via different authors and current study [10]

														$\Delta_{u,e}/\Delta_{u,P}$						
Sl.No.	Beam ID	Type of FRP rebar	b (mm)	d (mm)	D (mm)	L (mm)	a/d	ρ_f (%)	f'_c (MPa)	E_c (Gpa)	E_f (Gpa)	f_u (Mpa)	$P_{u,e}$ (kN)	$\Delta_{u,e}$ (mm)	Benmokrane [100]	Yost et al. [101]	Rafi & Nadjai [102]	Bischoff & Gross [103]	Adam et al. [104]	Kumar [99]	Job Thomas & S. Ramadass [4]
1	G6/0.5 [4]	GFRP	170	416	500	990	0,50	1,7	58,5	35,9	41,0	655	900	3,1	1,44	1,80	1,94	1,88	1,24	1,00	0,91
2	G6/0.75 [4]	GFRP	170	416	500	990	0,75	1,7	59	36,1	40,0	680	550	3,21	1,76	2,26	2,45	2,36	1,65	1,16	0,81
3	G6/1.0 [4]	GFRP	170	416	500	990	1,00	1,7	58	35,8	39,0	650	460	3,62	1,95	2,45	2,62	2,59	1,68	1,04	0,83
4	G4/0.5 [4]	GFRP	170	416	500	990	0,50	1,14	57,5	35,6	42,0	640	760	3,51	1,51	1,91	1,95	1,94	1,30	1,06	0,89
5	G4/0.75 [4]	GFRP	170	416	500	990	0,75	1,14	58	35,8	41,8	660	520	4,11	1,85	2,35	2,42	2,42	1,62	1,22	0,93
6	G4/1.0 [4]	GFRP	170	416	500	990	1,00	1,14	60	36,4	41,0	645	410	4,32	2,07	2,60	2,67	2,75	1,76	1,07	0,89
7	G1.13 [48]	GFRP	300	1088	1200	3000	1,15	1,21	37	28,6	66,4	1000	2687	22	2,45	2,94	2,94	3,00	1,79	1,58	1,67
8	G0.83 [48]	GFRP	300	1088	1200	2300	0,83	1,21	38,7	29,2	66,4	1000	3000	10,7	2,44	2,95	2,96	3,04	1,82	1,49	1,13
9	G1.47 [48]	GFRP	300	1088	1200	3700	1,47	1,21	38,7	59,2	66,4	1000	1849	29,1	2,88	3,48	3,50	3,54	2,17	1,61	1,64
10	A3D9M-1.4 [45]	AFRP	200	250	290	1500	1,40	0,38	26,1	24	80,6	1826,9	272,1	18,2	0,86	1,05	1,04	1,05	0,67	0,97	0,80
11	A3D9M-1.7 [45]	AFRP	200	250	290	1500	1,70	0,38	26,1	24	80,6	1826,9	197,9	22,74	1,27	1,57	1,55	1,57	1,02	1,28	1,00
12	A3D9M-2.1 [45]	AFRP	200	250	290	1500	2,10	0,38	26,1	24	80,6	1826,9	176	34,5	1,87	2,29	2,25	2,30	1,46	1,60	1,56
13	A4D9M-1.7 [45]	AFRP	200	250	290	1500	1,70	0,51	26,1	24	80,6	1826,9	242	26,8	1,55	1,89	1,85	1,90	1,19	1,63	1,47
14	A5D9M-1.7 [45]	AFRP	200	250	290	1500	1,70	0,64	26,1	24	80,6	1826,9	267,9	15,86	1,00	1,20	1,17	1,21	0,74	1,08	1,02
15	A5D9L-1.7 [45]	AFRP	200	310	350	1500	1,70	0,51	26,1	24	80,6	1826,9	268,5	16,7	1,43	1,75	1,72	1,76	1,11	1,25	1,34
16	C3D9M-1.4 [45]	CFRP	200	250	290	1500	1,40	0,38	26,1	24	120,2	1955,8	338,5	16,98	0,90	1,08	0,97	1,09	0,65	1,06	1,01
17	C3D9M-1.7 [45]	CFRP	200	250	290	1500	1,70	0,38	26,1	24	120,2	1955,8	213,1	13,62	0,98	1,19	1,07	1,20	0,74	1,04	0,80
18	C3D9M-2.1 [45]	CFRP	200	250	290	1500	2,10	0,38	26,1	24	120,2	1955,8	105,3	10,04	1,28	1,66	1,53	1,67	1,13	1,14	0,61
19	C4D9M-1.7 [45]	CFRP	200	250	290	1500	1,70	0,51	26,1	24	120,2	1955,8	192,2	12,98	1,30	1,59	1,45	1,62	1,01	1,46	0,94
20	C5D9M-1.7 [45]	CFRP	200	250	290	1500	1,70	0,64	26,1	24	120,2	1955,8	302,8	18,02	1,36	1,63	1,46	1,65	0,99	1,58	1,51
21	C5D9L-1.7 [45]	CFRP	200	310	350	1500	1,70	0,51	26,1	24	120,2	1955,8	290,8	16,66	1,81	2,18	1,96	2,22	1,34	1,66	1,70
22	A3D9S-1.7 [45]	AFRP	200	190	230	1500	1,70	0,50	26,1	24	80,6	1826,9	219,2	28,28	0,98	1,19	1,16	1,19	0,74	0,90	0,90
23	C3D9S-1.7 [45]	CFRP	200	190	230	1500	1,70	0,50	26,1	24	120,2	1955,8	209,7	18,34	0,91	1,10	0,99	1,11	0,68	1,20	0,80
24	G8N6 [42]	GFRP	300	1097	1200	3000	1,14	0,69	49,3	33	47,6	790	1447	12,4	1,38	1,71	1,74	1,80	1,09	0,79	0,73
25	G8N8 [42]	GFRP	300	1088	1200	3000	1,15	1,24	49,3	33	51,9	750	1906	12	1,65	2,00	2,07	2,11	1,25	0,97	0,87
26	C12N3 [42]	CFRP	300	1111	1200	3000	1,13	0,26	38,7	29,2	120	1596	1191	9,8	1,28	1,63	1,38	1,70	0,99	0,72	0,61
27	C12N4 [42]	CFRP	300	1106	1200	3000	1,13	0,46	38,7	29,2	144	1899	1601	10	1,71	2,10	1,80	2,20	1,30	0,98	0,79
28	A1N [44]	GFRP	310	257	306	1052	1,07	1,49	40,2	23	41,1	709	814	12,4	1,51	1,81	1,92	1,85	1,11	1,70	1,12
29	A2N [44]	GFRP	310	261	310	1252	1,44	1,47	45,4	22,9	41,1	709	471	11,3	1,31	1,58	1,69	1,64	1,00	1,39	0,69
30	A3N [44]	GFRP	310	261	310	1553	2,02	1,47	41,3	24,2	41,1	709	243	10,9	1,21	1,50	1,62	1,57	1,01	1,16	0,49
31	A4H [44]	GFRP	310	261	310	1553	2,02	1,47	64,6	22,5	41,1	709	192	9,5	1,35	1,75	1,87	2,01	1,29	1,27	0,34
32	B1N [44]	GFRP	300	503	608	1590	1,08	1,7	40,5	29,9	37,9	765	1273	9,1	1,36	1,66	1,79	1,69	1,07	1,20	0,70
33	B2N [44]	GFRP	300	501	606	1986	1,48	1,71	39,9	29,7	37,9	765	799	13,1	1,51	1,86	2,04	1,90	1,25	1,26	0,71
34	B3N [44]	GFRP	300	502	607	2580	2,07	1,71	41,2	30,2	37,9	765	431	15,3	1,46	1,88	2,13	1,92	1,42	1,13	0,53
35	B4N [44]	GFRP	300	496	606	1971	1,48	2,13	40,7	29,9	41,1	709	830	11,5	1,59	1,94	2,09	2,00	1,27	1,39	0,74
36	B5H [44]	GFRP	300	497	607	1971	1,48	2,12	66,4	38,3	41,1	709	1062	14,2	1,63	1,98	2,11	2,05	1,26	1,38	0,78
37	B6H [44]	GFRP	300	505	610	2580	2,06	1,7	68,5	38,9	37,9	765	376	12,9	1,65	2,29	2,62	2,37	2,03	1,12	0,38
38	C1N [44]	GFRP	301	889	1003	2448	1,10	1,58	51,6	33,8	42,3	938	2269	15,9	1,94	2,35	2,51	2,41	1,49	1,44	0,84
39	C2N [44]	GFRP	304	891	1005	3157	1,49	1,56	50,7	33,5	42,3	938	1324	18,3	1,76	2,17	2,35	2,25	1,45	1,25	0,66
40	C-0.7/1.6 [41]	CFRP	250	326	400	1600	1,69	0,78	40,5	29,9	143,0	1036	359	9,9	1,76	2,13	1,81	2,23	1,28	1,72	0,95
41	G-0.7/1.6 [41]	GFRP	250	326	400	1600	1,69	0,78	40,5	29,9	43,0	776	329	17,6	1,37	1,69	1,79	1,71	1,12	1,11	0,81
42	C-1.2/1.6 [41]	CFRP	250	326	400	1600	1,69	1,24	40,5	29,9	143,0	1036	390	8	1,79	2,17	1,86	2,26	1,32	1,89	0,96
43	G-1.2/1.6 [41]	GFRP	250	326	400	1600	1,69	1,24	40,5	29,9	43,0	776	350	12	1,26	1,55	1,67	1,59	1,04	1,10	0,76
44	C-1.7/1.6 [41]	CFRP	250	326	400	1600	1,69	1,71	40,5	29,9	143,0	1036	467	6,3	1,44	1,74	1,49	1,79	1,05	1,59	0,85
45	G-1.7/1.6 [41]	GFRP	250	326	400	1600	1,69	1,71	40,5	29,9	43,0	776	392	12	1,43	1,75	1,89	1,80	1,16	1,32	0,92
46	C-1.2/1.3 [41]	CFRP	250	326	400	1600	1,30	1,24	40,5	29,9	143,0	1036	744	10,6	1,51	1,80	1,55	1,84	1,08	1,90	1,28
47	G-1.2/1.3 [41]	GFRP	250	326	400	1600	1,30	1,24	40,5	29,9	43,0	776	538	13,7	1,12	1,36	1,45	1,38	0,88	1,19	0,86
48	CF-B-1 [39]	CFRP	150	150	200	950	1,55	1,13	34,7	27,7	134,0	1180	185,2	8,8	1,31	1,58	1,38	1,60	0,96	1,81	1,59
49	CF-d-250 [39]	CFRP	150	250	300	950	1,41	1,35	41,7	30,4	134,0	1180	298,1	8	2,96	3,56	3,10	3,62	2,14	2,47	2,08
50	CF-d-350 [39]	CFRP	150	350	400	950	1,36	1,21	37,6	28,8	134,0	1180	468,2	7,2	3,87	4,62	4,02	4,71	2,78	2,57	2,14
51	F-B-1 [39]	GFRP	150	150	200	950	1,55	1,29	35,5	28	40,8	690	135,5	14	1,33	1,62	1,75	1,64	1,06	1,50	1,34
52	F-d-250 [39]	GFRP	150	250	300	950	1,41	1,39	42	30,5	40,8	655	243,1	12	2,33	2,81	2,99	2,88	1,75	1,82	2,04
53	F-d-350 [39]	GFRP	150	350	400	950	1,36	1,24	48	32,6	40,8	655	422,5	7,8	1,99	2,39	2,53	2,45	1,45	0,91	1,63
Mean															1,62	1,98	1,97	2,04	1,28	1,34	1,03
S.D															0,55	0,66	0,64	0,68	0,42	0,37	0,42
CoV															33,9	33,3	32,5	33,3	32,8	27,6	40,8

The datas presented in this table are sourced from article number [10] in the literature.

Table 6: At ultimate (final) step, comparing experimental and predicted deflection in middle-span for test specimens via current application codes and current study [10]

														$\Delta_{u,e}/\Delta_{u,P}$				
Sl.No.	Beam ID	Type of FRP rebar	b (mm)	d (mm)	D (mm)	L (mm)	a/d	ρ_f (%)	f'_c (MPa)	Ec (Gpa)	E_f (Gpa)	f_p (Mpa)	$P_{u,e}$ (kN)	$\Delta_{u,e}$ (mm)	ACI 440.1R-06 [105]	ISIS-07 [94]	CAN/CSA-12 [98]	ACI 440.1R-15 [106]	Job Thomas & S. Ramadass [4]
1	G6/0.5 [4]	GFRP	170	416	500	990	0,50	1,7	58,5	35,9	41,0	655	900	3,1	1,85	1,75	1,67	1,82	0,91
2	G6/0.75 [4]	GFRP	170	416	500	990	0,75	1,7	59	36,1	40,0	680	550	3,21	2,34	2,14	2,03	2,26	0,81
3	G6/1.0 [4]	GFRP	170	416	500	990	1,00	1,7	58	35,8	39,0	650	460	3,62	2,50	2,37	2,29	2,57	0,83
4	G4/0.5 [4]	GFRP	170	416	500	990	0,50	1,14	57,5	35,6	42,0	640	760	3,51	1,87	1,76	1,63	1,84	0,89
5	G4/0.75 [4]	GFRP	170	416	500	990	0,75	1,14	58	35,8	41,8	660	520	4,11	2,31	2,16	2,04	2,3	0,93
6	G4/1.0 [4]	GFRP	170	416	500	990	1,00	1,14	60	36,4	41,0	645	410	4,32	2,54	2,41	2,32	2,65	0,89
7	G1.13 [48]	GFRP	300	1088	1200	3000	1,15	1,21	37	28,6	66,4	1000	2687	22	2,95	2,95	2,93	3,03	1,67
8	G0.83 [48]	GFRP	300	1088	1200	2300	0,83	1,21	38,7	29,2	66,4	1000	3000	10,7	2,96	2,96	2,92	3,07	1,13
9	G1.47 [48]	GFRP	300	1088	1200	3700	1,47	1,21	38,7	59,2	66,4	1000	1849	29,1	3,50	3,46	3,42	3,59	1,64
10	A3D9M-1.4 [45]	AFRP	200	250	290	1500	1,40	0,38	26,1	24	80,6	1826,9	272,1	18,2	1,07	1,04	1,02	1,05	0,8
11	A3D9M-1.7 [45]	AFRP	200	250	290	1500	1,70	0,38	26,1	24	80,6	1826,9	197,9	22,74	1,60	1,53	1,50	1,57	1,00
12	A3D9M-2.1 [45]	AFRP	200	250	290	1500	2,10	0,38	26,1	24	80,6	1826,9	176	34,5	2,32	2,25	2,21	2,31	1,56
13	A4D9M-1.7 [45]	AFRP	200	250	290	1500	1,70	0,51	26,1	24	80,6	1826,9	242	26,8	1,92	1,87	1,85	1,90	1,47
14	A5D9M-1.7 [45]	AFRP	200	250	290	1500	1,70	0,64	26,1	24	80,6	1826,9	267,9	15,86	1,22	1,20	1,18	1,21	1,02
15	A5D9L-1.7 [45]	AFRP	200	310	350	1500	1,70	0,51	26,1	24	80,6	1826,9	268,5	16,7	1,77	1,73	1,70	1,77	1,34
16	C3D9M-1.4 [45]	CFRP	200	250	290	1500	1,40	0,38	26,1	24	120,2	1955,8	338,5	16,98	1,08	1,07	1,06	1,09	1,01
17	C3D9M-1.7 [45]	CFRP	200	250	290	1500	1,70	0,38	26,1	24	120,2	1955,8	213,1	13,62	1,19	1,18	1,16	1,20	0,80
18	C3D9M-2.1 [45]	CFRP	200	250	290	1500	2,10	0,38	26,1	24	120,2	1955,8	105,3	10,04	1,68	1,56	1,51	1,65	0,61
19	C4D9M-1.7 [45]	CFRP	200	250	290	1500	1,70	0,51	26,1	24	120,2	1955,8	192,2	12,98	1,61	1,58	1,55	1,62	0,94
20	C5D9M-1.7 [45]	CFRP	200	250	290	1500	1,70	0,64	26,1	24	120,2	1955,8	302,8	18,02	1,64	1,63	1,62	1,65	1,51
21	C5D9L-1.7 [45]	CFRP	200	310	350	1500	1,70	0,51	26,1	24	120,2	1955,8	290,8	16,66	2,19	2,18	2,16	2,23	1,70
22	A3D9S-1.7 [45]	AFRP	200	190	230	1500	1,70	0,50	26,1	24	80,6	1826,9	219,2	28,28	1,20	1,17	1,16	1,19	0,90
23	C3D9S-1.7 [45]	CFRP	200	190	230	1500	1,70	0,50	26,1	24	120,2	1955,8	209,7	18,34	1,11	1,10	1,08	1,11	0,80
24	G8N6 [42]	GFRP	300	1097	1200	3000	1,14	0,69	49,3	33	47,6	790	1447	12,4	1,67	1,64	1,59	1,79	0,73
25	G8N8 [42]	GFRP	300	1088	1200	3000	1,15	1,24	49,3	33	51,9	750	1906	12	2,00	2,01	1,97	2,13	0,87
26	C12N3 [42]	CFRP	300	1111	1200	3000	1,13	0,26	38,7	29,2	120	1596	1191	9,8	1,51	1,53	1,48	1,67	0,61
27	C12N4 [42]	CFRP	300	1106	1200	3000	1,13	0,46	38,7	29,2	144	1899	1601	10	2,08	2,09	2,04	2,22	0,79
28	A1N [44]	GFRP	310	257	306	1052	1,07	1,49	40,2	23	41,1	709	814	12,4	1,82	1,82	1,80	1,85	1,12
29	A2N [44]	GFRP	310	261	310	1252	1,44	1,47	45,4	22,9	41,1	709	471	11,3	1,60	1,59	1,56	1,64	0,69
30	A3N [44]	GFRP	310	261	310	1553	2,02	1,47	41,3	24,2	41,1	709	243	10,9	1,54	1,48	1,43	1,56	0,49
31	A4H [44]	GFRP	310	261	310	1553	2,02	1,47	64,6	22,5	41,1	709	192	9,5	1,79	1,71	1,60	1,80	0,34
32	B1N [44]	GFRP	300	503	608	1590	1,08	1,7	40,5	29,9	37,9	765	1273	9,1	1,69	1,64	1,62	1,69	0,70
33	B2N [44]	GFRP	300	501	606	1986	1,48	1,71	39,9	29,7	37,9	765	799	13,1	1,93	1,83	1,79	1,91	0,71
34	B3N [44]	GFRP	300	502	607	2580	2,07	1,71	41,2	30,2	37,9	765	431	15,3	2,03	1,78	1,73	1,91	0,53
35	B4N [44]	GFRP	300	496	606	1971	1,48	2,13	40,7	29,9	41,1	709	830	11,5	1,99	1,93	1,89	2,01	0,74
36	B5H [44]	GFRP	300	497	607	1971	1,48	2,12	66,4	38,3	41,1	709	1062	14,2	2,01	1,97	1,94	2,06	0,78
37	B6H [44]	GFRP	300	505	610	2580	2,06	1,7	68,5	38,9	37,9	765	376	12,9	2,52	1,95	1,85	2,09	0,38
38	C1N [44]	GFRP	301	889	1003	2448	1,10	1,58	51,6	33,8	42,3	938	2269	15,9	2,39	2,35	2,31	2,43	0,84
39	C2N [44]	GFRP	304	891	1005	3157	1,49	1,56	50,7	33,5	42,3	938	1324	18,3	2,25	2,14	2,10	2,27	0,66
40	C-0.7/1.6 [41]	CFRP	250	326	400	1600	1,69	0,78	40,5	29,9	143,0	1036	359	9,9	2,09	2,14	2,09	2,23	0,95
41	G-0.7/1.6 [41]	GFRP	250	326	400	1600	1,69	0,78	40,5	29,9	43,0	776	329	17,6	1,71	1,61	1,57	1,70	0,81
42	C-1.2/1.6 [41]	CFRP	250	326	400	1600	1,69	1,24	40,5	29,9	143,0	1036	390	8	2,16	2,19	2,15	2,27	0,96
43	G-1.2/1.6 [41]	GFRP	250	326	400	1600	1,69	1,24	40,5	29,9	43,0	776	350	12	1,60	1,51	1,47	1,59	0,76
44	C-1.7/1.6 [41]	CFRP	250	326	400	1600	1,69	1,71	40,5	29,9	143,0	1036	467	6,3	1,74	1,75	1,73	1,79	0,85
45	G-1.7/1.6 [41]	GFRP	250	326	400	1600	1,69	1,71	40,5	29,9	43,0	776	392	12	1,80	1,73	1,70	1,80	0,92
46	C-1.2/1.3 [41]	CFRP	250	326	400	1600	1,30	1,24	40,5	29,9	143,0	1036	744	10,6	1,80	1,81	1,80	1,84	1,28
47	G-1.2/1.3 [41]	GFRP	250	326	400	1600	1,30	1,24	40,5	29,9	43,0	776	538	13,7	1,38	1,34	1,32	1,38	0,86
48	CF-B-1 [39]	CFRP	150	150	200	950	1,55	1,13	34,7	27,7	134,0	1180	185,2	8,8	1,58	1,58	1,56	1,60	1,59
49	CF-d-250 [39]	CFRP	150	250	300	950	1,41	1,35	41,7	30,4	134,0	1180	298,1	8	3,54	3,57	3,54	3,65	2,08
50	CF-d-350 [39]	CFRP	150	350	400	950	1,36	1,21	37,6	28,8	134,0	1180	468,2	7,2	4,62	4,65	4,62	4,77	2,14
51	F-B-1 [39]	GFRP	150	150	200	950	1,55	1,29	35,5	28	40,8	690	135,5	14	1,66	1,59	1,55	1,63	1,34
52	F-d-250 [39]	GFRP	150	250	300	950	1,41	1,39	42	30,5	40,8	655	243,1	12	2,83	2,8	2,76	2,91	2,04
53	F-d-350 [39]	GFRP	150	350	400	950	1,36	1,24	48	32,6	40,8	655	422,5	7,8	2,39	2,39	2,37	2,51	1,63
Mean															2,00	1,95	1,90	2,03	1,03
S.D															0,66	0,66	0,66	0,69	0,42
CoV															33,0	33,9	34,7	33,99	40,8

The datas presented in this table are sourced from article number [10] in the literature.

Table 7: Comparison of Ultimate Load Determination Formula Proposed in NSM Section with Other Formulas and Studies [10]

															$P_{u,e}$ / $P_{u,p}$							
Sl.No.	Beam ID	Type of FRP rebar	b (mm)	d (mm)	D (mm)	L(mm)	(a/d)	ρ_f (%)	f'_c (MPa)	Ec (Gpa)	E_f (Gpa)	f_f (Mpa)	$P_{u,e}$ (kN)	NSM (equa. 39)	JSCE [95]	BISE [96]	NRC [97]	ISIS [94]	ACI 318 [43]	CSA [98]	Job Thomas & S. Ramadass [4]	$P_{u,e}$/NSM
1	G6/0.5 [4]	GFRP	170	416	500	990	0,5	1,7	58,5	35,9	41	655	900	407,86	10.09	8,08	7,7	9,18	1,33	1,71	1,19	2,21
2	G6/0.75 [4]	GFRP	170	416	500	990	0,75	1,7	59	36,1	40	680	550	331,55	6.21	4,97	4,74	5,66	0,81	1,05	1,08	1,66
3	G6/1.0 [4]	GFRP	170	416	500	990	1	1,7	58	35,8	39	650	460	258,61	5.24	4,21	4,05	4,83	0,69	0,89	1,14	1,78
4	G4/0.5 [4]	GFRP	170	416	500	990	0,5	1,14	57,5	35,6	42	640	760	330,15	9.65	7,78	7,35	7,74	1,14	1,62	1,12	2,30
5	G4/0.75 [4]	GFRP	170	416	500	990	0,75	1,14	58	35,8	41,8	660	520	267,48	6.61	5,32	5,02	5,28	0,78	1,11	1,14	1,94
6	G4/1.0 [4]	GFRP	170	416	500	990	1	1,14	60	36,4	41	645	410	210,96	5.25	4,17	3,93	4,13	0,59	0,87	1,11	1,94
7	G1.13 [48]	GFRP	300	1088	1200	3000	1,15	1,21	37	28,6	66,4	1000	2687	974,97	8.55	7,39	6,5	5,87	1,69	2,7	1,62	2,8
8	G0.83 [48]	GFRP	300	1088	1200	2300	0,83	1,21	38,7	29,2	66,4	1000	3000	1301,84	9.40	8,12	7,1	6,41	1,33	2,41	1,36	2,30
9	G1.47 [48]	GFRP	300	1088	1200	3700	1,47	1,21	38,7	59,2	66,4	1000	1849	730,17	5.80	5,01	4,38	3,95	1,42	2,64	1,30	2,53
10	A3D9M-1.4 [45]	AFRP	200	250	290	1500	1,4	0,38	26,1	24	80,6	1827	272,1	99,87	6.07	5,24	4,28	4,19	1,04	1,74	1,15	2,72
11	A3D9M-1.7 [45]	AFRP	200	250	290	1500	1,7	0,38	26,1	24	80,6	1827	197,9	76,16	4.41	3,81	3,12	3,05	0,93	1,7	0,98	2,60
12	A3D9M-2.1 [45]	AFRP	200	250	290	1500	2,1	0,38	26,1	24	80,6	1827	176	53,06	4.90	3,39	2,77	2,71	1,05	2,07	1,05	3,32
13	A4D9M-1.7 [45]	AFRP	200	250	290	1500	1,7	0,51	26,1	24	80,6	1827	242	88,23	4.90	4,22	3,67	3,72	1,09	1,9	1,18	2,74
14	A5D9M-1.7 [45]	AFRP	200	250	290	1500	1,7	0,64	26,1	24	80,6	1827	267,9	98,84	5.04	4,33	3,92	4,12	1,16	1,97	1,29	2,71
15	A5D9L-1.7 [45]	AFRP	200	310	350	1500	1,7	0,51	26,1	24	80,6	1827	268,5	106,48	4.62	3,99	3,44	3,34	1,08	1,73	1,26	2,52
16	C3D9M-1.4 [45]	CFRP	200	250	290	1500	1,4	0,38	26,1	24	120,2	1956	338,5	103,33	6.61	5,7	4,37	4,27	1,22	1,93	1,41	3,28
17	C3D9M-1.7 [45]	CFRP	200	250	290	1500	1,7	0,38	26,1	24	120,2	1956	213,1	78,80	4.16	3,59	2,75	2,69	0,94	1,63	1,03	2,70
18	C3D9M-2.1 [45]	CFRP	200	250	290	1500	2,1	0,38	26,1	24	120,2	1956	105,3	54,90	2.06	1,77	1,36	1,33	0,59	1,1	0,61	1,92
19	C4D9M-1.7 [45]	CFRP	200	250	290	1500	1,7	0,51	26,1	24	120,2	1956	192,2	91,29	3.41	2,94	2,39	2,43	0,81	1,34	0,92	2,11
20	C5D9M-1.7 [45]	CFRP	200	250	290	1500	1,7	0,64	26,1	24	120,2	1956	302,8	102,26	4.99	4,29	3,63	3,82	1,23	1,98	1,43	2,96
21	C5D9L-1.7 [45]	CFRP	200	310	350	1500	1,7	0,51	26,1	24	120,2	1956	290,8	110,18	4.38	3,78	3,05	2,96	1,09	1,66	1,32	2,64
22	A3D9S-1.7 [45]	AFRP	200	190	230	1500	1,7	0,5	26,1	24	80,6	1827	219,2	69,29	5.48	4,73	4,2	4,44	1,12	2,28	1,47	3,16
23	C3D9S-1.7 [45]	CFRP	200	190	230	1500	1,7	0,5	26,1	24	120,2	1956	209,7	71,69	4.59	3,96	3,29	3,48	1,02	1,94	1,05	2,93
24	G8N6 [42]	GFRP	300	1097	1200	3000	1,14	0,69	49,3	33	47,6	790	1447	660,33	5.71	4,84	4,05	3,21	0,74	1,69	1,09	2,19
25	G8N8 [42]	GFRP	300	1088	1200	3000	1,15	1,24	49,3	33	51,9	750	1906	854,75	6.04	5,13	4,49	4,08	0,98	1,86	1,22	2,23
26	C12N3 [42]	CFRP	300	1111	1200	3000	1,13	0,26	38,7	29,2	120	1596	1191	581,36	5.04	4,35	2,65	1,85	0,77	1,51	1,02	2,05
27	C12N4 [42]	CFRP	300	1106	1200	3000	1,13	0,46	38,7	29,2	144	1899	1601	843,50	5.29	4,57	3,08	2,29	1,04	1,63	1,13	1,90
28	A1N [44]	GFRP	310	257	306	1052	1,07	1,49	40,2	23	41,1	709	814	255,74	7.88	6,81	6,87	8,89	1	1,55	1,12	3,18
29	A2N [44]	GFRP	310	261	310	1252	1,44	1,47	45,4	22,9	41,1	709	471	184,22	4.35	3,76	3,71	4,77	0,66	1,33	0,75	2,56
30	A3N [44]	GFRP	310	261	310	1553	2,02	1,47	41,3	24,2	41,1	709	243	109,08	2.31	2	2,01	2,58	0,55	1,17	0,55	2,23
31	A4H [44]	GFRP	310	261	310	1553	2,02	1,47	64,6	22,5	41,1	709	192	109,08	1.76	1,36	1,27	1,63	0,28	0,8	0,34	1,76
32	B1N [44]	GFRP	300	503	608	1590	1,08	1,7	40,5	29,9	37,9	765	1273	545,56	7.54	6,52	6,88	7,61	0,8	1,62	0,92	2,33
33	B2N [44]	GFRP	300	501	606	1986	1,48	1,71	39,9	29,7	37,9	765	799	379,95	4.76	4,12	4,35	4,83	0,68	1,64	0,75	2,10
34	B3N [44]	GFRP	300	502	607	2580	2,07	1,71	41,2	30,2	37,9	765	431	223,32	2.54	2,19	2,31	2,56	0,52	1,44	0,52	1,93
35	B4N [44]	GFRP	300	496	606	1971	1,48	2,13	40,7	29,9	41,1	709	830	408,24	4.48	3,87	3,97	4,82	0,69	1,55	0,75	2,03
36	B5H [44]	GFRP	300	497	607	1971	1,48	2,12	66,4	38,3	41,1	709	1062	407,95	5.48	4,21	3,98	4,82	0,54	1,68	0,76	2,60
37	B6H [44]	GFRP	300	505	610	2580	2,06	1,7	68,5	38,9	37,9	765	376	225,80	2.12	1,61	1,56	1,72	0,27	1,05	0,35	1,67
38	C1N [44]	GFRP	301	889	1003	2448	1,1	1,58	51,6	33,8	42,3	938	2269	945,87	8.24	6,88	6,53	6,42	0,68	2,14	0,87	2,40
39	C2N [44]	GFRP	304	891	1005	3157	1,49	1,56	50,7	33,5	42,3	938	1324	666,88	4.77	4,01	3,82	3,73	0,53	1,97	0,64	1,99
40	C-0.7/1.6 [41]	CFRP	250	326	400	1600	1,69	0,78	40,5	29,9	143	1036	359	141,15	2.94	2,54	1,98	2,05	0,59	1,17	0,79	2,54
41	G-0.7/1.6 [41]	GFRP	250	326	400	1600	1,69	0,78	40,5	29,9	43	776	329	122,16	4.03	3,48	3,31	3,42	0,63	1,51	0,81	2,69
42	C-1.2/1.6 [41]	CFRP	250	326	400	1600	1,69	1,24	40,5	29,9	143	1036	390	177,97	2.74	2,37	1,92	2,22	0,64	1,1	0,80	2,19
43	G-1.2/1.6 [41]	GFRP	250	326	400	1600	1,69	1,24	40,5	29,9	43	776	350	154,03	3.67	3,17	3,14	3,64	0,58	1,4	0,83	2,27
44	C-1.7/1.6 [41]	CFRP	250	326	400	1600	1,69	1,71	40,5	29,9	143	1036	467	209,00	2.95	2,55	2,07	2,66	0,77	1,19	0,91	2,23
45	G-1.7/1.6 [41]	GFRP	250	326	400	1600	1,69	1,71	40,5	29,9	43	776	392	180,88	3.69	3,19	3,17	4,07	0,64	1,42	0,90	2,17
46	C-1.2/1.3 [41]	CFRP	250	326	400	1600	1,3	1,24	40,5	29,9	143	1036	744	253,16	5.23	4,52	3,66	4,24	0,97	1,42	1,23	2,94
47	G-1.2/1.3 [41]	GFRP	250	326	400	1600	1,3	1,24	40,5	29,9	43	776	538	219,10	5.64	4,88	4,83	5,59	0,7	1,46	1,03	2,46
48	CF-B-1 [39]	CFRP	150	150	200	950	1,55	1,13	34,7	27,7	134	1180	185,2	58,18	4.77	3,72	3,32	4,27	0,9	1,73	1,45	3,18
49	CF-d-250 [39]	CFRP	150	250	300	950	1,41	1,35	41,7	30,4	134	1180	298,1	108,25	5.12	3,62	2,98	3,76	1,12	1,29	1,33	2,75
50	CF-d-350 [39]	CFRP	150	350	400	950	1,36	1,21	37,6	28,8	134	1180	468,2	142,96	6.73	4,75	3,94	4,44	1,9	1,57	1,13	3,28
51	F-B-1 [39]	GFRP	150	150	200	950	1,55	1,29	35,5	28	40,8	690	135,5	47,53	3.72	3,84	4,19	5,6	0,65	1,73	1,16	2,85
52	F-d-250 [39]	GFRP	150	250	300	950	1,41	1,39	42	30,5	40,8	655	243,1	81,84	5.50	4,34	4,36	5,53	0,91	1,5	1,39	2,97
53	F-d-350 [39]	GFRP	150	350	400	950	1,36	1,24	48	32,6	40,8	655	422,5	107,82	4.63	5,82	5,66	6,42	1,34	1,86	1,93	3,92
Mean															5.13	4,34	3,91	4,21	0,89	1,6	1,05	2,48
S.D															1.88	1,57	1,54	1,76	0,32	0,41	0,31	0,48
CoV															36.6	36,2	39,4	41,7	36,3	25,6	29,5	19,57

The datas presented in this table are sourced from article number [10] in the literature.

Table 8: Comparison of Ultimate Deflection Determination Formula Proposed in NSM Section with Other Formulas and Studies [10]

															$\Delta_{u,e}/\Delta_{u,P}$										
Sl.No.	Beam ID	Type of FRP rebar	b (mm)	d (mm)	D (mm)	L (mm)	(a/d)	ρ_f (%)	f'_c (MPa)	Ec (Gpa)	E_f (Gpa)	f_u (Mpa)	$\Delta_{u,e}$ (mm)	NSM (equa. 40)	ACI 440.1R-06 [40]	ISIS-07 [28]	CAN/CSA-12 [32]	ACI 440.1R-15 [41]	Benmokrane [35]	Yost et al. [36]	Rafi & Nadjai [37]	Bischoff & Gross [38]	Adam et al. [39]	Job Thomas & S. Ramadass [10]	$\Delta_{u,e}$/NSM
1	G6/0.5 [4]	GFRP	170	416	500	990	0,5	1,7	58,5	35,9	41	655	3,1	5,5	1,85	1,75	1,67	1,82	1,44	1,80	1,94	1,88	1,24	0,91	0,56
2	G6/0.75 [4]	GFRP	170	416	500	990	0,75	1,7	59	36,1	40	680	3,21	5,58	2,34	2,14	2,03	2,26	1,76	2,26	2,45	2,36	1,65	0,81	0,58
3	G6/1.0 [4]	GFRP	170	416	500	990	1	1,7	58	35,8	39	650	3,62	5,69	2,50	2,37	2,29	2,57	1,95	2,45	2,62	2,59	1,68	0,83	0,64
4	G4/0.5 [4]	GFRP	170	416	500	990	0,5	1,14	57,5	35,6	42	640	3,51	5,84	1,87	1,76	1,63	1,84	1,51	1,91	1,95	1,94	1,30	0,89	0,60
5	G4/0.75 [4]	GFRP	170	416	500	990	0,75	1,14	58	35,8	41,8	660	4,11	5,83	2,31	2,16	2,04	2,3	1,85	2,35	2,42	2,42	1,62	0,93	0,71
6	G4/1.0 [4]	GFRP	170	416	500	990	1	1,14	60	36,4	41	645	4,32	5,75	2,54	2,41	2,32	2,65	2,07	2,6	2,67	2,75	1,76	0,89	0,75
7	G1.13 [48]	GFRP	300	1088	1200	3000	1,15	1,21	37	28,6	66,4	1000	22	13,21	2,95	2,95	2,93	3,03	2,45	2,94	2,94	3,00	1,79	1,67	1,67
8	G0.83 [48]	GFRP	300	1088	1200	2300	0,83	1,21	38,7	29,2	66,4	1000	10,7	9,20	2,96	2,96	2,92	3,07	2,44	2,95	2,96	3,04	1,82	1,13	1,16
9	G1.47 [48]	GFRP	300	1088	1200	3700	1,47	1,21	38,7	59,2	66,4	1000	29,1	28,33	3,50	3,46	3,42	3,59	2,88	3,48	3,5	3,54	2,17	1,64	1,03
10	A3D9M-1.4 [45]	AFRP	200	250	290	1500	1,4	0,38	26,1	24	80,6	1827	18,2	19,70	1,07	1,04	1,02	1,05	0,86	1,05	1,04	1,05	0,67	0,80	0,92
11	A3D9M-1.7 [45]	AFRP	200	250	290	1500	1,7	0,38	26,1	24	80,6	1827	22,74	19,70	1,60	1,53	1,5	1,57	1,27	1,57	1,55	1,57	1,02	1,00	1,15
12	A3D9M-2.1 [45]	AFRP	200	250	290	1500	2,1	0,38	26,1	24	80,6	1827	34,5	19,70	2,32	2,25	2,21	2,31	1,87	2,29	2,25	2,30	1,46	1,56	1,75
13	A4D9M-1.7 [45]	AFRP	200	250	290	1500	1,7	0,51	26,1	24	80,6	1827	26,8	18,99	1,92	1,87	1,85	1,9	1,55	1,89	1,85	1,90	1,19	1,47	1,41
14	A5D9M-1.7 [45]	AFRP	200	250	290	1500	1,7	0,64	26,1	24	80,6	1827	15,86	18,45	1,22	1,2	1,18	1,21	1	1,2	1,17	1,21	0,74	1,02	0,86
15	A5D9L-1.7 [45]	AFRP	200	310	350	1500	1,7	0,51	26,1	24	80,6	1827	16,7	17,00	1,77	1,73	1,7	1,77	1,43	1,75	1,72	1,76	1,11	1,34	0,98
16	C3D9M-1.4 [45]	CFRP	200	250	290	1500	1,4	0,38	26,1	24	120,2	1956	16,98	16,96	1,08	1,07	1,06	1,09	0,9	1,08	0,97	1,09	0,65	1,01	1,00
17	C3D9M-1.7 [45]	CFRP	200	250	290	1500	1,7	0,38	26,1	24	120,2	1956	13,62	16,96	1,19	1,18	1,16	1,2	0,98	1,19	1,07	1,20	0,74	0,80	0,80
18	C3D9M-2.1 [45]	CFRP	200	250	290	1500	2,1	0,38	26,1	24	120,2	1956	10,04	16,96	1,68	1,56	1,51	1,65	1,28	1,66	1,53	1,67	1,13	0,61	0,59
19	C4D9M-1.7 [45]	CFRP	200	250	290	1500	1,7	0,51	26,1	24	120,2	1956	12,98	16,34	1,61	1,58	1,55	1,62	1,3	1,59	1,45	1,62	1,01	0,94	0,79
20	C5D9M-1.7 [45]	CFRP	200	250	290	1500	1,7	0,64	26,1	24	120,2	1956	18,02	15,89	1,64	1,63	1,62	1,65	1,36	1,63	1,46	1,65	0,99	1,51	1,13
21	C5D9L-1.7 [45]	CFRP	200	310	350	1500	1,7	0,51	26,1	24	120,2	1956	16,66	14,63	2,19	2,18	2,16	2,23	1,81	2,18	1,96	2,22	1,34	1,70	1,14
22	A3D9S-1.7 [45]	AFRP	200	190	230	1500	1,7	0,5	26,1	24	80,6	1827	28,28	21,77	1,20	1,17	1,16	1,19	0,98	1,19	1,16	1,19	0,74	0,90	1,30
23	C3D9S-1.7 [45]	CFRP	200	190	230	1500	1,7	0,5	26,1	24	120,2	1956	18,34	18,74	1,11	1,1	1,08	1,11	0,91	1,1	0,99	1,11	0,68	0,80	0,98
24	GBN6 [42]	GFRP	300	1097	1200	3000	1,14	0,69	49,3	33	47,6	790	12,4	13,44	1,67	1,64	1,59	1,79	1,38	1,71	1,74	1,80	1,09	0,73	0,92
25	GBN8 [42]	GFRP	300	1088	1200	3000	1,15	1,24	49,3	33	51,9	750	12	12,07	2,00	2,01	1,97	2,13	1,65	2	2,07	2,11	1,25	0,87	0,99
26	C12N3 [42]	CFRP	300	1111	1200	3000	1,13	0,26	38,7	29,2	120	1596	9,8	12,52	1,51	1,53	1,48	1,67	1,28	1,63	1,38	1,70	0,99	0,61	0,78
27	C12N4 [42]	CFRP	300	1106	1200	3000	1,13	0,46	38,7	29,2	144	1899	10	10,87	2,08	2,09	2,04	2,22	1,71	2,1	1,8	2,20	1,30	0,79	0,92
28	A1N [44]	GFRP	310	257	306	1052	1,07	1,49	40,2	23	41,1	709	12,4	7,43	1,82	1,82	1,8	1,85	1,51	1,81	1,92	1,85	1,11	1,12	1,67
29	A2N [44]	GFRP	310	261	310	1252	1,44	1,47	45,4	22,9	41,1	709	11,3	8,10	1,60	1,59	1,56	1,64	1,31	1,58	1,69	1,64	1,00	0,69	1,39
30	A3N [44]	GFRP	310	261	310	1553	2,02	1,47	41,3	24,2	41,1	709	10,9	12,15	1,54	1,48	1,43	1,56	1,21	1,5	1,62	1,57	1,01	0,49	0,90
31	A4H [44]	GFRP	310	261	310	1553	2,02	1,47	64,6	22,5	41,1	709	9,5	7,36	1,79	1,71	1,6	1,8	1,35	1,75	1,87	2,01	1,29	0,34	1,29
32	B1N [44]	GFRP	300	503	608	1590	1,08	1,7	40,5	29,9	37,9	765	9,1	9,98	1,69	1,64	1,62	1,69	1,36	1,66	1,79	1,69	1,07	0,70	0,91
33	B2N [44]	GFRP	300	501	606	1986	1,48	1,71	39,9	29,7	37,9	765	13,1	13,32	1,93	1,83	1,79	1,91	1,51	1,86	2,04	1,90	1,25	0,71	0,98
34	B3N [44]	GFRP	300	502	607	2580	2,07	1,71	41,2	30,2	37,9	765	15,3	18,10	2,03	1,78	1,73	1,91	1,46	1,88	2,13	1,92	1,42	0,53	0,85
35	B4N [44]	GFRP	300	496	606	1971	1,48	2,13	40,7	29,9	41,1	709	11,5	12,24	1,99	1,93	1,89	2,01	1,59	1,94	2,09	2,00	1,27	0,74	0,94
36	B5H [44]	GFRP	300	497	607	1971	1,48	2,12	66,4	38,3	41,1	709	14,2	9,03	2,01	1,97	1,94	2,06	1,63	1,98	2,11	2,05	1,26	0,78	1,57
37	B6H [44]	GFRP	300	505	610	2580	2,06	1,7	68,5	38,9	37,9	765	12,9	13,13	2,52	1,95	1,85	2,09	1,65	2,29	2,62	2,37	2,03	0,38	0,98
38	C1N [44]	GFRP	301	889	1003	2448	1,1	1,58	51,6	33,8	42,3	938	15,9	10,60	2,39	2,35	2,31	2,43	1,94	2,35	2,51	2,41	1,49	0,84	1,50
39	C2N [44]	GFRP	304	891	1005	3157	1,49	1,56	50,7	33,5	42,3	938	18,3	14,70	2,25	2,14	2,1	2,27	1,76	2,17	2,35	2,25	1,45	0,66	1,25
40	C-0.7/1.6 [41]	CFRP	250	326	400	1600	1,69	0,78	40,5	29,9	143	1036	9,9	9,12	2,09	2,14	2,09	2,23	1,76	2,13	1,81	2,23	1,28	0,95	1,09
41	G-0.7/1.6 [41]	GFRP	250	326	400	1600	1,69	0,78	40,5	29,9	43	776	17,6	14,32	1,71	1,61	1,57	1,7	1,37	1,69	1,79	1,71	1,12	0,81	1,23
42	C-1.2/1.6 [41]	CFRP	250	326	400	1600	1,69	1,24	40,5	29,9	143	1036	8	8,61	2,16	2,19	2,15	2,27	1,79	2,17	1,86	2,26	1,32	0,96	0,93
43	G-1.2/1.6 [41]	GFRP	250	326	400	1600	1,69	1,24	40,5	29,9	43	776	12	13,51	1,60	1,51	1,47	1,59	1,26	1,55	1,67	1,59	1,04	0,76	0,89
44	C-1.7/1.6 [41]	CFRP	250	326	400	1600	1,69	1,71	40,5	29,9	143	1036	6,3	8,27	1,74	1,75	1,73	1,79	1,44	1,74	1,49	1,79	1,05	0,85	0,76
45	G-1.7/1.6 [41]	GFRP	250	326	400	1600	1,69	1,71	40,5	29,9	43	776	12	12,98	1,80	1,73	1,7	1,8	1,43	1,75	1,89	1,80	1,16	0,92	0,92
46	C-1.2/1.3 [41]	CFRP	250	326	400	1600	1,3	1,24	40,5	29,9	143	1036	10,6	8,61	1,80	1,81	1,8	1,84	1,51	1,8	1,55	1,84	1,08	1,28	1,23
47	G-1.2/1.3 [41]	GFRP	250	326	400	1600	1,3	1,24	40,5	29,9	43	776	13,7	13,51	1,38	1,34	1,32	1,38	1,12	1,36	1,45	1,38	0,88	0,86	1,01
48	CF-B-1 [39]	CFRP	150	150	200	950	1,55	1,13	34,7	27,7	134	1180	8,8	8,80	1,58	1,58	1,56	1,6	1,31	1,58	1,38	1,60	0,96	1,59	1,00
49	CF-d-250 [39]	CFRP	150	250	300	950	1,41	1,35	41,7	30,4	134	1180	8	6,12	3,54	3,57	3,54	3,65	2,96	3,56	3,1	3,62	2,14	2,08	1,31
50	CF-d-350 [39]	CFRP	150	350	400	950	1,36	1,21	37,6	28,8	134	1180	7,2	5,59	4,62	4,65	4,62	4,77	3,87	4,62	4,02	4,71	2,78	2,14	1,29
51	F-B-1 [39]	GFRP	150	150	200	950	1,55	1,29	35,5	28	40,8	690	14	13,32	1,66	1,59	1,55	1,63	1,33	1,62	1,75	1,64	1,06	1,34	1,05
52	F-d-250 [39]	GFRP	150	250	300	950	1,41	1,39	42	30,5	40,8	655	12	9,48	2,83	2,8	2,76	2,91	2,33	2,81	2,99	2,88	1,75	2,04	1,27
53	F-d-350 [39]	GFRP	150	350	400	950	1,36	1,24	48	32,6	40,8	655	7,8	7,48	2,39	2,39	2,37	2,51	1,99	2,39	2,53	2,45	1,45	1,63	1,04
Mean															2,00	1,95	1,9	2,03	1,62	1,98	1,97	2,04	1,28	1,03	1,04
S.D															0,7	0,66	0,7	0,69	0,55	0,66	0,64	0,68	0,42	0,42	0,28
CoV															33,0	33,9	34,7	34,0	33,9	33,3	32,5	33,30	32,80	40,80	26,99

The datas presented in this table are sourced from article number [10] in the literature.

References

[1] Abed F, Elchabib H, Alhamaydeh M. Shear characteristics of GFRP-reinforced concrete deep beams without web reinforcement. Journal of Reinforced Plastics and Composites 2012;31(13):1063–1073.
[2] Dhahir MK. Strut and tie modeling of deep beams shear strengthened with FRP laminates. Composite Structures 2018; 193:247–259.
[3] Farghaly AS, Benmokrane B. Shear behavior of FRP-reinforced concrete deep beams without web reinforcement. Journal of Composites for Construction 2013;17(4):04013015–040130210.
[4] Baghi H, Barros JA, Kaszubska M, Kotynia R. Shear behavior of concrete beams reinforced exclusively with longitudinal glass fiber reinforced polymer bars: Analytical model. Structural Concrete 2018;19(1):162–173.
[5] Ayman M. Composites: Construction materials for the new era. In: Advanced Polymer Composites for Structural Applications in Construction (ACIC), Venice, Italy; 2004. p. 45–58.
[6] International Federation for Structural Concrete (fib). Bulletin 40: FRP reinforcement for RC structures. 2007.
[7] Yavuz G. Lif takviyeli polimerlerin betonarme kirişlerde donatı olarak kullanımı. e-Journal of New World Sciences Academy 2011;6(4):1A0212:1001–1015.
[8] Numerical analysis of AFRP reinforced concrete columns with replaceable structural fuses as energy dissipaters under cyclic loading. In: Proceedings of the Structures Congress 2018, Fort Worth, TX, USA. doi:10.1061/9780784481332.029.
[9] Lu WY, Hwang SJ, Lin IJ. Deflection prediction for reinforced concrete deep beams. Computers and Concrete 2010;7(1):1–16.
[10] Thomas J, Ramadass S. Prediction of the load and deflection response of concrete deep beams reinforced with FRP bars. Mechanics of Advanced Materials and Structures 2019. doi:10.1080/15376494.2018.1549292.
[11] Nehdi M, Omeman Z, El-Chabib H. Optimal efficiency factor in strut-and-tie model for FRP-reinforced concrete short beams with (1.5 < a/d < 2.5). Materials and Structures 2008; 41:1713–1727.
[12] El-Sayed AK, El-Salakawy EF, Benmokrane B. Shear strength of fibre-reinforced polymer reinforced concrete deep beams without web reinforcement. Canadian Journal of Civil Engineering 2012;39(5):546–555.
[13] Farghaly AS, Benmokrane B. Shear behavior of FRP-reinforced concrete deep beams without web reinforcement. Journal of Composites for Construction 2013;5(4):268–275.
[14] Andermatt MF, Lubell AS. Behavior of concrete deep beams reinforced with internal fiber-reinforced polymer—Experimental study. ACI Structural Journal 2013;110(4):585–594.
[15] Kim D, Lee J, Lee YH. Effectiveness factor of strut-and-tie models for concrete deep beams reinforced with FRP rebars. Composites Part B: Engineering 2014;56:117–125.
[16] Mohamed K. Performance and strut efficiency factor of concrete deep beams reinforced with GFRP bars. Ph.D. thesis. Sherbrooke: University of Sherbrooke; 2015.
[17] IS 1343. Code of Practice for Prestressed Concrete (1st Revision). New Delhi: Bureau of Indian Standards; 1980.
[18] Dischinger F. Contribution to the theory of the half disc and the wall-like wearer. International Association of Bridge and Structural Engineering 1932;1:69–93.
[19] IS 456. Plain and Reinforced Concrete, Code of Practice (4th Revision). New Delhi: Bureau of Indian Standards; 2000.
[20] Hwang SJ, Lee HJ. Strength prediction for discontinuity regions by softened strut-and-tie model. Journal of Structural Engineering 2002;128(12):1519–1526.
[21] Hsu TTC. Toward a unified nomenclature for reinforced concrete theory. Journal of Structural Engineering 1996;122(3):275–283. [Also see discussion by Mo YL, Hsu TTC. Journal of Structural Engineering 1997;123(12):1691–1693.]
[22] Hwang SJ, Lee HJ. Analytical model for predicting shear strengths of exterior reinforced concrete beam-column joint for seismic resistances. ACI Structural Journal 1999;96(5):846–857.

[23] Hwang SJ, Lu WY, Lee HJ. Shear strength prediction for deep beams. ACI Structural Journal 2000;97(3):367–376.
[24] Hwang SJ, Lu WY, Lee HJ. Shear strength prediction for reinforced concrete corbels. ACI Structural Journal 2000;97(4):543–552.
[25] Hwang SJ, Fang WH, Lee HJ, Yu HW. Analytical model for predicting shear strengths of squat walls. Journal of Structural Engineering 2001;127(1):43–50.
[26] Zhang LXB, Hsu TTC. Behavior and analysis of 100 MPa concrete membrane elements. Journal of Structural Engineering 1998;124(1):24–34.
[27] British Standards Institution. British Standard Code of Practice for the Structural Use of Concrete. P:110, Part-I, 14–16. London: BSI; 1972.
[28] Canadian Network of Centres of Excellence on Intelligent Sensing for Innovative Structures (ISIS). Reinforcing concrete structures with fibre reinforced polymers. ISIS-M03-07; 2007.
[29] Japan Society of Civil Engineers (JSCE). Recommendations for design and construction of concrete structures using continuous fibre reinforced materials. Concrete Engineering Series, No. 23. Tokyo: JSCE; 1997.
[30] British Institution of Structural Engineers (BISE). Interim guidance on the design of reinforced concrete structures using fibre composite reinforcement. London: BISE; 1999.
[31] National Research Council (NRC). Guide for the design and construction of concrete structures reinforced with fiber-reinforced polymer bars. CNR-DT-203-NRC-06. Ottawa: NRC; 2006.
[32] Canadian Standards Association. Design and Construction of Building Structures with Fibre-reinforced Polymers (CAN/CSA S806-11). Ontario: CSA; 2011.
[33] American Concrete Institute (ACI). Building code requirements for structural concrete and commentary (ACI 318-08). Farmington Hills, MI: ACI; 2008.
[34] Kumar P. Short-term deflection of deep beams. ACI Journal 1978;75(8):381–383.
[35] Benmokrane B, Challal O, Masmoudi R. Flexural response of concrete beams reinforced with FRP reinforcing bar. ACI Structural Journal 1996;93(1):46–55.
[36] Yost JR, Gross SP, Dinehart DW. Effective moment of inertia for glass fiber-reinforced polymer-reinforced concrete beams. ACI Structural Journal 2003;100(6):732–739.
[37] Rafi MM, Nadjai A. Evaluation of ACI 440 deflection model for fiber-reinforced polymer reinforced concrete beams and suggested modification. ACI Structural Journal 2009;106(6):762–771.
[38] Bischoff PH, Gross SP. Equivalent moment of inertia based on integration of curvature. Journal of Composites for Construction 2011;15(3):263–273.
[39] Adam MA, Said M, Mahmoud AA, Shanour AS. Analytical and experimental flexural behaviour of concrete beams reinforced with glass fiber reinforced polymer bars. Construction and Building Materials 2015; 84:354–366.
[40] ACI Committee 440. Guide for the Design and Construction of Structural Concrete Reinforced with FRP Bars (ACI 440.1R-06). Farmington Hills, MI: ACI; 2006.
[41] ACI Committee 440. Guide for the Design and Construction of Structural Concrete Reinforced with Fiber Reinforced Polymer (FRP) Bars (ACI 440.1R-15). Farmington Hills, MI: ACI; 2015.